Green synthesis and transport properties of ZnS-PPy hybrid nanocomposites.

Kousik Dutta
Department of Physics, Behala College, Parnashree; Kolkata- 700060; INDIA
(Dated: October 20, 2017)

The development of green synthesis route through biological method for the synthesis of nanoparticles using plants have received attention in the recent times as it is environment friendly and economical method. ZnS nanoparticles have been prepared using glucose both as capping agent and stabilizer. The mean particle size of the ZnS nanoparticles is found to be 5.8 nm. Inorganic-organic hybrid nanocomposites are synthesized by dispersing nanosized ZnS in the conducting polypyrrole matrix. The samples are characterized by X-ray diffraction, transmission and scanning electron microscopes and UV-VIS spectrophotometer. The wavelength of optical absorption peak of ZnS nanoparticle increases from 265 nm to 283 nm with the decrease of polypyrrole concentration. Studies on dc electrical conductivity as a function of temperature suggest that three dimensional Mott's hopping process occurs in ZnS - polypyrrole nanocomposites. The observed non linear current-voltage characteristics are satisfactorily explained using the Schottky type barriers.

PACS numbers:

I. INTRODUCTION

The fabrication of complex nanoarchitechtures with controlled morphology, orientation and dimensionality have attracted significant attention over the past two decades since such controlled is crucial for the determination structure property relationship in many process, development of new path ways for the material synthesis, and novel application of nanostructured materials.[1–4] A great deal of work has been done in the past two decades with regard to the ZnS[5], CdS,[6] CdTe[7] and an investigation of their optical properties. ZnS nanoparticle being a wide band gap (bulk band gap =3.6 eV) semiconductor, are good emitters of light in blue and ultraviolet range which has found many application in flat panel display[8], photocatalysis[9] and electroluminescent devices.[10]

High surface to volume ratio allows ZnS nanoparticles are ideally suited for applications in biological systems due to much less toxicity as compared to other II-VI nanoparticles such as CdS, CdTe. The electronic properties of nanosized ZnS are also strongly influenced by doping of transition and rare earth metals.[11,12] The emission efficiency and thermal stability are increased upon reduction of ZnS particle size.[13–15] Most of the previous work on ZnS low dimensional systems reported different ZnS nanostructured like nanoparticles, nanorods, etc. either in powder form or suspended in colloids. For example, one dimensional ZnS nanostructures have been reported, including ZnS nanowires by liquid crystal template, micelle template, thermal evaporation using Au catalyst etc. ZnS nanobelts via thermal evaporation method without any catalyst was also reported. But there is a growing concern towards use of these chemicals as they are reported to be very toxic for the environment. Apart from the toxicity, these chemical based methods are also not cost effective, a major disadvantage for synthesis of nanoparticles at the industrial scale. Due to these problems, various eco-friendly approaches for the synthesis of ZnS nanoparticles are being adopted. Among them, plants and plant extracts seem to be the best option because they are cost efficient and require little or no maintenance. A vast repertoire of secondary metabolites is found in all plants which possess redox capacity and can be exploited for biosynthesis of nanoparticles. As a wide range of metabolites are presented in the plant, the nanoparticles produced by using plants are more stable and the rate of synthesis is faster in comparison to microorganism.

Glucose is a simple monosaccharide found in plants whose five hydroxyl groups are arranged in a specific way along its sixcarbon backbone. The use of carbohydrates for the synthesis of nanomaterials has recently become an active research area. Gole A et al used glucose as a reductant to prepare gold nanoparticles. Raveendran P et al used D-glucose as the reducing agent and starch as a capping agent to prepare Ag nanoparticles. Power M. J. et al and Bansal P. et al used glucose as a capping agent for the synthesis of CdS[16,17]. In this paper it is reporting a simple and economical method for the preparation of ZnS nanoparticles using glucose as a capping agent. Glucose has been selected as the capping agent because it is abundant, natural, renewable and biodegradable. Since it is biodegradable, it may also help in reducing cytotoxicity problem of nano materials, a major limitation for their biological applications and could extend the applications of ZnS nanoparticles to food and pharmaceutical product.

The combination of inorganic and organic species generate new materials for the development of new multifunctional devices. The integration of inorganic and organic components is performed by insertion of organic molecules into inorganic host matrix. Hybrid II-VI semiconductor nanocomposites are formed through chemical bonding with organic substance.[18–20] Dispersion of inorganic nanoparticles in the polymer matrix is a novel route to synthesize hybrid inorganic-organic nanocomposites. Conducting polymers have attracted significant attention because of their potential application in various field.[21,22]

The nanocomposite of metal and semiconductor particles are important in several optical and electrical application and their preparation in polymeric matrices with significant errors on the ability to controlled the size and morphology via organometallic route is highly challenging. The conductivity of conducting polymers can be varied by several orders of magnitude by changing doping compounds and preparation conditions.[23,24] Intrinsically conducting polymer like polypyrrole, polyaniline have potential for wide variety of application in electronic system etc, because of their high electrical conductivity, good environmental stability and ease of preparation. Mutual interactions between inorganic semiconductor and organic polymers may give rise to interesting properties which are significantly different from individual components. Electronic properties of nanosized materials are strongly dependent on the environment. Main aim of this paper is to concentrate to investigate the optical properties and current-voltage characteristics of nanoscale ZnS embedded in conducting polypyrrole matrix.

II. EXPERIMENTAL

All the chemicals used were of analytical grade. Pyrrole (AR grade)and ammonium peroxydisulphate (APS) ($(NH_4)_2S_2O_8$) were obtained from E. Merck (India). Pyrrole(AR grade) was purified and stored at -15^{0}C in a refrigerator prior to use. APS oxidant was used as received.

$Zn(NO_3)_2$ and Na_2S are used as Zinc source and Sulphur source respectively. $Zn(NO_3)_2$, Na_2S and glucose are obtained from E. Merck. These are of high purity and used without any future purification. In Zn $(NO_3)_2(1M)$ solution, Na_2S (1M) solution is added drop wise with continuous stirring. A white coloured solution is formed which is further shaken on a magnetic stirrer for 15 hours. Now, 1.0M glucose solution is added drop wise in this white coloured solution. The resultant solution is heated and incubated for 6 hours. Precipitates obtained are centrifuged with 2,000 rpm for 15 mints. The final product is dried at 200C for 4 hours and then crushed to fine powder. This zinc sulphide nanoparticles was used to prepare PPY/ZnS nanocomposites

The required quantity of ZnS nanoparticle was ultrasonically dispersed in 50 ml deionized water. Pyrrole monomer of known volume was slowly added into the dispersion under sonication at room temperature. After 45 minutes APS solution maintaining Pyrrole : APS mole ratio of 1:1.25 was added drop wise to well dispersed suspension mixture for 2 hour with a continuous stirring. The solution turned black after some time . The resulting black dispersion were centrifuged at 8000 r.p.m for 1 hour using high speed centrifuge instrument. The supernatant were carefully decanted and discarded and the resulting black sediments were redispersed in water. Different compositions of nanocomposite samples by varying the amount of pyrrole (polypyrrole) were prepared as shown in Table I. The samples were pressed into pellets of diameter 1 cm. The thickness of the samples varies from 0.10 cm to 0.12 cm. Compositions of different nanocomposite samples were prepared as shown in Table I.

X ray diffraction pattern of the nanocomposites were performed using a Philips Difractrometer(PW1710) with Cu kα radiation. Scanning electron microscope (SEM)(Model JEOL JSM6700F) image was obtained using scanning electron microscope. Transmission electron micrographs were taken from JEOL, JEM 2010. UV-visible spectra of the diluted nanocomposite dispersions in the 200-1000 nm range were obtained using Perkins-Elmer instrument. The temperature dependent dc conductivity was measured by the standard four-probe method using Keithley digital multimeter (Keithley 2000 programmable multimeter). The room temperature current-voltage (I-V) characteristics were measured by Keithley 220 programmable current source meter. The electrical contacts were made by silver paint.

III. RESULTS AND DISCUSSION

Figure 1 displays the powder X-ray diffraction (XRD) of the sample S4. The wide angle XRD pattern for the bulk system exhibits three distinct peaks in the range of 2θ = 25 -60 ^{0}, characteristics of the cubic structure. The peaks are fairly broad suggesting the nanostructure of ZnS. The three strong peaks appeared at angles (2θ) of 28.7, 47.7, 56.6 correspond to 111, 220 and 311 planes of cubic ZnS. Two crystalline polymorphs of ZnS are found: cubic zincblende (saphlerite) and hexagonal (wurtzite). Cubic phase is the most stable phase at ambient condition. Hexagonal structure is formed at highest temperature (>1200 K). The present XRD pattern matches well with the reported cubic phase of ZnS. The mean size (D) of ZnS nanoparticles of the nanocomposite is calculated following the Scherrer's equation[25]

$$D = K\lambda/\beta\cos\theta \quad (1)$$

where K = 0.89, D represents coherent length, λ, the wavelength of $CuK\alpha$ radiation and β, the corrected value at full width at half maxima (FWHM) of the diffraction peak. At 2θ= 28.7^o, which is the characteristics peak of ZnS, is chosen to calculate D. The estimated size of nanocrystalline ZnS is 5 nm.

Figures 2(a)-(b) show the TEM micrograph of the ZnS-polypyrrole nanocomposites sample S4. Figure 2(a) indicates the diffraction pattern of the nanocomposite sample and it consists of several concentric rings. From the diameter of the rings, it is calculated the inter planer spacing values values which correspond to reflection from 111, 220 and 311 planes of cubic ZnS. From the figure 2(b) it is obtained the nanocomposite particle are nearly spherical crystallites in shape. The mean particle size of nanocomposite ZnS particles are in the ranging of 5-10 nm which is good agreement with XRD result.

The scanning electron micrograph (SEM) of the nanocomposite sample S4 is shown in Figure 3. The nanocomposite particles are well dispersed and are of spherical shape with uniform diameter lying in the range from 10 - 20 nm. Larger particle size may be due to the aggregation of smaller particles in the presence of polymer matrix.

Figure 4 shows FTIR spectra of the nanocomposite sample S1. The band at 1552 cm^{-1} corresponds to typical pyrrole rings vibration. The peak at 1467 cm^{-1} is attributed to = CH in plane vibration and peaks at 921 cm^{-1} and 793 cm^{-1} due to = CH out of plane vibration. The characteristic bands at 1310 cm^{-1}, 1190 cm^{-1}, 1050 cm^{-1} and 664 cm^{-1} are related to C-H and N-H in-plane and bending vibrations. The very strong peak at 1120^{-1} may be contributed by - C - O groups of glucose(here this band overlap with strong band 1190 cm^{-1}). The peaks at 3500^{-1} is very broad and strong and can be assigned to the OH groups from glucose. The IR study confirms the presence of C-O and OH groups of glucose have a strong ability to bind metal . The characteristics bands of bare PPY are 1551 cm^{-1}, 1440 cm^{-1}, 921 cm^{-1}, 788 cm^{-1}, corresponding to pyrrole rings, in and out of plane = CH vibrations. Almost all the bands reveal blue shift in the nanocomposites which indicates that there is a strong interaction between polypyrrole and ZnS nanoparticles.

The variation of room temperature conductivity $\sigma(RT)$ with the weight percentage of pyrrole are shown in Table I. The conductivity increases with the increasing content of pyrrole. Electrical conductivity of ZnS is very low due to wide band gap. The enhancement of $\sigma(RT)$ is about one order of magnitude for the highest fraction of pyrrole. Much higher room temperature conductivity of the nanocomposites indicates that electrical conduction is dominated by the pyrrole. The temperature dependence of conductivity for all samples are shown in Figure 5. Conducting pyrrole behaves like disordered semiconductors.[24] Thus the variation of conductivity $\sigma(T)$ with temperature can be described by three dimensional Mott's variable range hopping (VRH) model,[26]

$$\sigma(T) = \sigma_0 exp(-(\frac{T_0}{T})^{\frac{1}{4}}) \tag{2}$$

where σ_0 is the high temperature limit of conductivity and T_0 is Mott's characteristic temperature associated with the degree of localization of the electronic wave function. The values of Mott's characteristic temperature T_0 and the pre exponential factor σ_0 are obtained from the slopes and intercepts of the Figure 5 and are given in Table I. The calculated values of T_0 and σ_0 increase with the increase of ZnS content.

The Mott's characteristic temperature T_0 for three dimensional hopping transport is given by,

$$T_0 = 16/(kL^3 N(E_F)), \tag{3}$$

where L is the localization length and $N(E_F)$ is the density of states at the Fermi level. The values of $N(E_F)$ are calculated by considering the charge transport primarily arising from conducting pyrrole phase and assuming localization length of the pyrrole monomer unit about 3 Å.[27,28] The higher values of density of states at the Fermi level are found with increase of pyrrole content.

The average hopping distance R_{hop} between two sites and the activation energy W_{hop} are

$$R_{hop} = (3/8)(T_0/T)^{\frac{1}{4}} L \tag{4}$$

$$W_{hop} = (1/4)kT(T_0/T)^{\frac{1}{4}} \tag{5}$$

At room temperature the average hopping distance varies from 17 Åto 26 Åfor as shown in Table I. This corresponds to about 5 - 8 monomer units in length. The estimated activation energies for hopping as shown in Table I are in the range of 106 - 139 meV. In case of in situ polymerization of pyrrole in the presence of ZnS nanoparticles, monomer is adsorbed on the surface of nanoparticle. The growth of pyrrole depends on the concentration of ZnS. The increase of ZnS amount reduces the conjugation length of polymer. The conductivity of conjugated polymers critically depends on its conjugation length. It is observed that the conductivity decreases with decreasing conjugation length.[29] Moreover ZnS is less conducting than pyrrole. As a results of it, the conductivity of nanocomposites decreases with increasing weight percentage of ZnS.

Electronic UV-Vis absorption spectra of nanocomposite S1, S2, S3, S4 are shown in the Figure 6. Electronic absorption spectra of pure ZnS nanoparticle is dipicted in the inset of the Figure 6. The absorbtion spectra reveal three absorption bands in the entire wavelength range. Out of these three bands, one sharp peak is observed around 260 - 285 nm and two broad peaks at 400-1000 nm. Different spectroscopic techniques[30] and theoretical energy band calculation[31] indicate that the absorbtion band at 400 - 500 nm (3-2.5 eV) is assigned to $\pi - \pi^*$ transition of polypyrrole. Upon doping PPY exhibits unusual electronic structure due to electron-phonon coupling. The absorption peak associated with ZnS are found in the wavelength range 260-285 nm as shown in Table 2. The excitonic peaks for all the samples are well shifted from absorption peak at 345 nm[32] for bulk ZnS. The reduction of size in semiconductor reveals a blue shift due to quantum size effect. The dramatic modifications of electronic absorption bands of individual ZnS and PPY suggest that nanosized ZnS are incorporated into polypyrrole matrix.

The optical band gap E_g is related to the absorption coefficient α by the relation[33]

$$\alpha = \frac{B(h\nu - E_g)^{1/2}}{h\nu} \tag{6}$$

where B is the absorption constant for a direct transition. For allowed direct transition one can plot $(\alpha h\nu)^2$ vs. $h\nu$ and extrapolate the linear portion of it to $\alpha = 0$ value to

obtain the corresponding band gap. The plots of $(\alpha h\nu)^2$ vs. hν for the sample S4 are presented in Figure 7. The calculated band gaps of ZnS in the nanocomposites are 4.67 eV, 4.55 eV, 4.42 eV and 4.26 eV for S1, S2, S3 and S4 respectively.

Quantum size effects on electronic energy bands of semiconductors become prominent when the size of nanocrystallites is less than bulk exciton Bohr radius. Coulomb interaction between hole and electron plays crucial role in nanosized solids. The quantum confinement of charge carriers modifies valence and conduction bands of semiconductors. The band gap shift ΔE_g with respect to the bulk value based on effective mass approximation can be estimated from the equation[34,35]

$$(\Delta\, E_g) = E_g(nano) - E_g(bulk) = [\hbar^2\pi^2/2\mu r^2] - [1.8e^2/\epsilon r] \quad (7)$$

where $\mu = m_e{}^* m_h{}^* / (m_e{}^* + m_h{}^*)$ is the reduced electron hole effective mass, $m_e{}^*$ and $m_h{}^*$ are the effective masses of electron and hole , respectively. ϵ is the dielectric constant of the material. The diameter has been calculated assuming the effective masses[36] $m_e{}^* = 0.42 m_0$, $m_h{}^* = 0.61 m_0$, m_0 is the free electron mass and the dielectric constant[37] $\epsilon = 8.76$. The estimated size of pure ZnS using Eqation 7 is about 6 nm which is in good agreement with our experimental results.

Figure 8 shows the current vs voltage (I-V) characteristics of the sample S4 at room temperature. Current versus voltage characteristics are asymmetric and nonlinear for forward and reverse directions of applied voltage. This suggests that Schottky barriers are formed in the nanocomposites. The applied forward bias and the current based on thermionic emission current can be written as[38]

$$I_f = I_0(exp[\frac{qV}{nkT}] - 1) \quad (8)$$

Where n is the ideality factor, I_0 is the saturation current and defined by

$$I_0 = AA^*T^2 exp[-\frac{q\Phi}{kT}] \quad (9)$$

where the quantities A, A*, T, q, k and Φ are the area, the effective Richardson constant, temperature in Kelvin, the electronic charge, Boltzmann constant and the apparent barrier height. The current density J is obtained from the geometrical area. The variation of current density, J with forward voltage is shown in Figure 9. The values of saturation current density J_0 and n are determined from the non linear curve fitting to equation (8) as shown in Figure 9. The calculated values of J_0 and n for all the samples S1, S2, S3 and S4 are shown in Table II.

The voltage dependance of the reverse current can be written as[38],

$$I_r = Iexp[\frac{\beta V^{1/2}}{kT}] \quad (10)$$

where

$$I = AA^*T^2 exp[-\frac{\Phi}{kT}] \quad (11)$$

where β is related to the barrier height. The linear behavior in plot of the current density J vs. $V^{1/2}$ as depicted in Figure 10 indicates that the I-V characteristics are consistent with equation (10). The estimated values of β for are shown in Table II. Saturation current density and ideality factor decrease while β increases with increase of PPY amount. The non-linear I-V characteristics are observed in polycrystalline ZnS ceramics. The Schottky type energy barrier at the grain boundaries are observed. Polypyrrole influences the surface and vacancy states of nanocrystalline ZnS which leads to nonlinear behavior in I-V characteristics.

IV. CONCLUSION

The shifting of optical absorption band of ZnS in the nanocomposites reveals the interaction with polypyrrole matrix. Electrical conduction originates from polypyrrole and obeys three dimensional hopping mechanism. The frequency dependent conductivity confirms the correlated barrier hopping of charge carriers. The modification of microstructure of nanocomposites and electronic properties of ZnS and polypyrrole lead to a variation of barrier height with the composition.

[1] J.T. Hu, T.W. Odom and C.M. Lieber, J. Am. Chem. Soc. **32**, 435 (1999).
[2] M. Law, J. Goldberg, and P.D. Yang, Annu. Rev. Mater. Res, **34**, 83 (2004).
[3] J.K. Yuan, W.N. Li, S. Goldberg and S.L. Suib, J. Am. Chem. Soc. **127**, 14184 (2005).
[4] B. Liu and H.C. Zeng, J. Am. Chem. Soc. **126**, 8124 (2004).
[5] A.K. Dinsmore, D.S. Hsu, H.F. Gray, S.B. Quadri, Y. Tian, B.R. Ratna, Appl. Phys. Lett. **75**, 802 (1999).
[6] J. Tittle, W. Gohde, F. Koberling, Th Basche, A. Kornowski, H. Weller, A. Eychmuller, J. Phys. chem. B. **101**, 3013 (1997).
[7] A.L. Rogach, Mater. sci. Eng. B. **69-70**, 435 (2000).
[8] R. Vacassy, S.M. Scholz, J. Dutta, H. Hofmann, C.J.G. Plummer, G. Carrot, J. Hilborn, M. Akine, Mater. Res. Soc. Symp. proc. **501**, 369 (1998)
[9] C. L. Torres- Martinez, R. Kho, O.I. Mian, R.K. Mehra, colloid. J. Int erf. sci. **240**, 525 (2001)
[10] P. Calandra, M. Goffredi, L. Turco, Colloids Surf. A. **160**, 9 (1999)
[11] Y.Q. Li, J.A. Zapien, Y.Y. Shan, Y.K. Liu and S.T. Lee, Appl. Phys. Letts. **88**, 013115 (2006).

[12] S. Sapra, A. Prakash, A. Ghangrekar, N. Periasamy and D. D. Sarma, J. Phys. Chem. B **109**, 1663 (2005).
[13] R.N. Bhargava and D. Gallagher, Phys. Rev. Lett. **72**, 416 (1994).
[14] A.A. Bol and A. Meijerink, J. Phys. Chem. B, **105**, 10203 (2001).
[15] Y. Zhang and Y. Li, J. Phys. Chem. B,**108**, 17805 (2004) .
[16] Pawer M.J. and Chaure S.S, **12**, 689-693 (2009)
[17] Bansal P., Jaggi N. and Rohilla S.K., Res.J.Chem.Sci., **2**, 69-71 (2012)
[18] X. Huang, H. R.Heulings, V. Le and J. Li, Chem. Mater. **13**, 3754 (2001).
[19] H.R. Heullings, X. Huang, J. Li, T. Yuen and C.L. Lin, Nano Lett, **1**, 521 (2001).
[20] L. Fan, H. Song, H. Zhao, C. Pan, H. Yu, X. Bai, S. Li, Y. Lei, Q. Dai, R. Qin, T. wang, B. Dong, Z. Zheng and X. Ren , J. Phys. Chem. B, **110**, 12948 (2006).
[21] A. Tiwari, R.Kumar, M.Prabhakaran, R.R. Pandey, P. Kumari, A. Chadurvedi, A. K. Mishra, Polymers for Advanced Technologies, **21**, 615 (2010).
[22] A. Tiwari, M. Prabaharan, R. Pandey, S. Li, Journal of Inorganic and Organometallic Polymers and Materials, **20(2)**, 380 (2010).
[23] A.J. Heeger, Rev. Mod. Physics. **73**, 681 (2001).
[24] T. Skotheim and R. Elsenbaumer, Handbook of Conducting Polymers, Marcel Dekker, New York, 1998.
[25] H. P. Klug and L. E. Alexander, X-ray diffraction procedures for polycrystalline and amorphous materials, John Wiley and Sons, New York, 1954, P491.
[26] N.F. Mott, E. Davis, Electronic Process in Non Crystalline Materials, 2nd ed., Oxford, Clarendon, 1979
[27] D.S. Maddison and T.L. Tansley, J. of Appl. Phys. **72**, 4677 (1992)
[28] B.R. Saunders, K.S. Murray and R.J. Fleming, Synth. Met. **47**, 167 (1992)
[29] S. Roth, H. Bleier and W. Pukacki, Faraday Discuss. Che. Soc. **88**, 223 (1989)
[30] P. Batz, D. Schmeisser, W. Gopel, Phys. Rev. B, **43**, 9178 (1991)
[31] J. L. Bredas, J. C. Scott, K. Yakushi, G. B. Street, Phys. Rev. B **30**, 1023 (1984)
[32] Introduction to Solid State Physics. Kittel, C., Ed.; Wiley: New York, 1986; Chapter 8.
[33] J. I. Pankove, Optical Processes in Semiconductors, Prentice Hall, New Jersy, 1971
[34] L.E. Brus, J. Chem. Phys. **80**, 4403 (1984)
[35] Y. Kayanuma Phys. Rev. B **38**, 9797 (1988)
[36] P.E. Lippeens and M. Lannoo, Phys. Rev. B. **39**, 10935 (1989)
[37] E.O. Kane, Phys. Rev. B. **18**, 6849 (1978)
[38] S.M. Sze, Physics of Semiconductor Devices, John Wiley and Sons, Berlin, New York, 1981

TABLE I: Weight percentage of Polypyrrole (x%), room temperature dc conductivity (σ_{RT}), σ_0, T_0, density of states $N(E_F)$, hopping length R_{hop} , activation energy W_{hop}

Sample	x	σ_{RT} (10^{-3}) (S/cm)	$\sigma_0(10^4)$ (S/cm)	$T_0(10^7)$ (K)	$N(E_F)(10^{21})$ ($eV^{-1}cm^{-3}$)	R_{hop} (Å)	W_{hop} (meV)
S1	85	5.42	1.20	1.37	1.51	17	106
S2	75	3.37	8.84	2.51	0.82	20	110
S3	65	2.35	23.09	3.44	0.62	22	118
S4	55	0.87	106.65	5.76	0.35	26	139

TABLE II: Absorption wavelength on ZnS-PPY solution, Saturation current density J_0, Ideality factor n and Barrier height β.

Sample	λ_{peak} (nm)	$J_0(10^{-7})$ (A-cm^{-2})	n	β
S1	265 [a]	24.56	12.95	5.25
S2	272 [a]	15.65	17.80	4.25
S3	275 [a]	8.45	23.25	3.34
S4	283 [a]	4.45	28.25	1.25

[a] ZnS band.

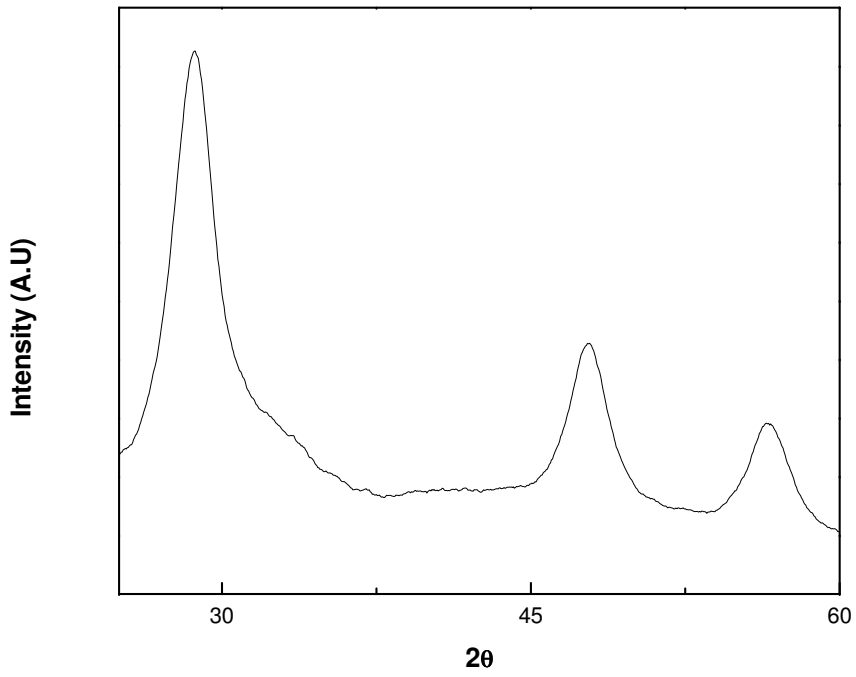

FIG. 1: X-ray diffraction pattern of ZnS-PPY nanocomposites sample S4.

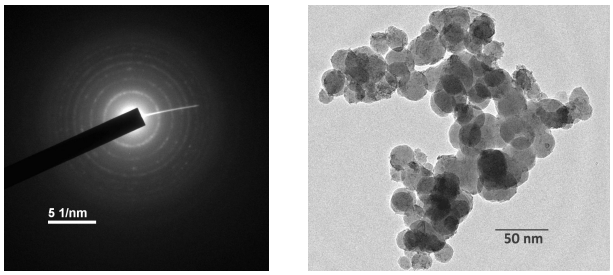

FIG. 2: TEM micrograph of (a) diffraction pattern of ZnS (b) lower magnification image of nanocomposites sample S4.

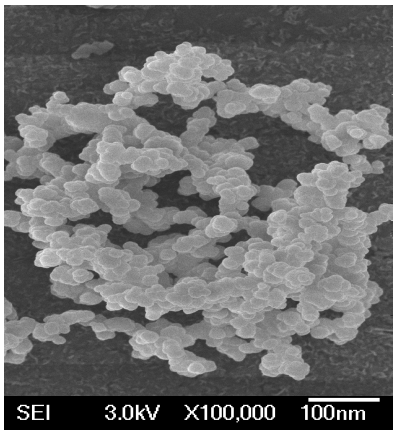

FIG. 3: Scanning Electron Micrograph (SEM) of nanocomposite sample S4.

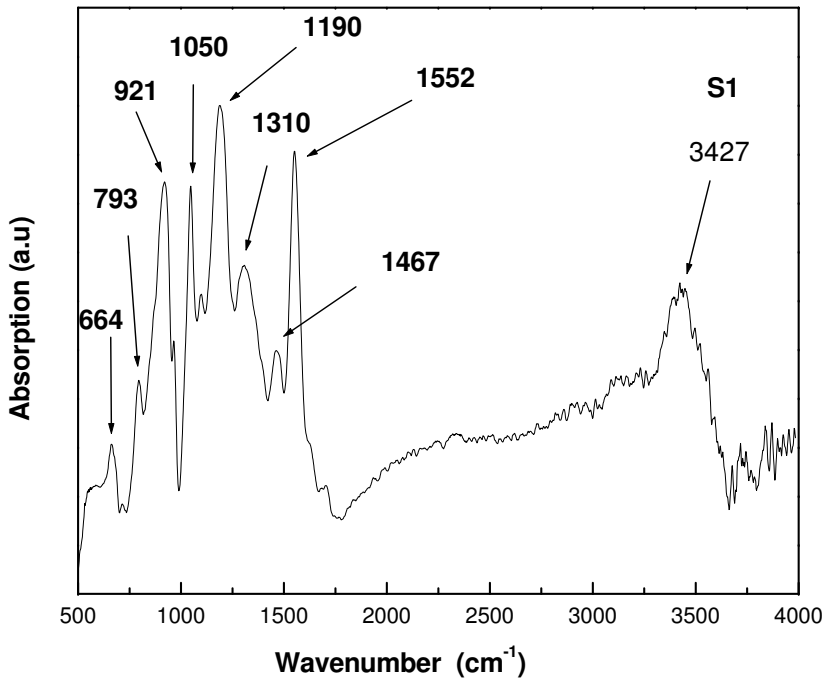

FIG. 4: Fourier Transform Infrared (FTIR) spectra of sample S1.

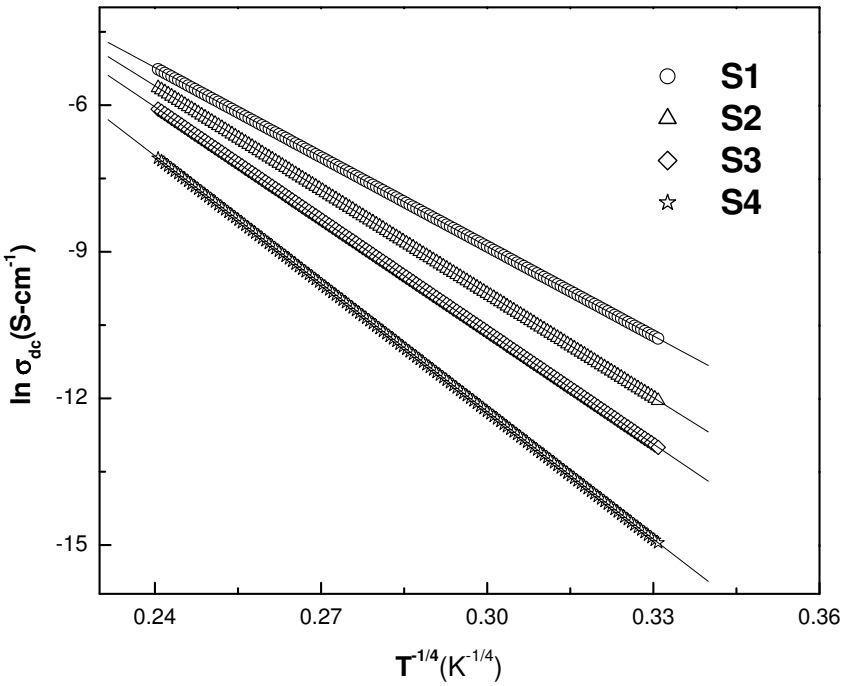

FIG. 5: Temperature variation of dc conductivity of the nanocomposites. The solid lines are fits to Eq.(2)

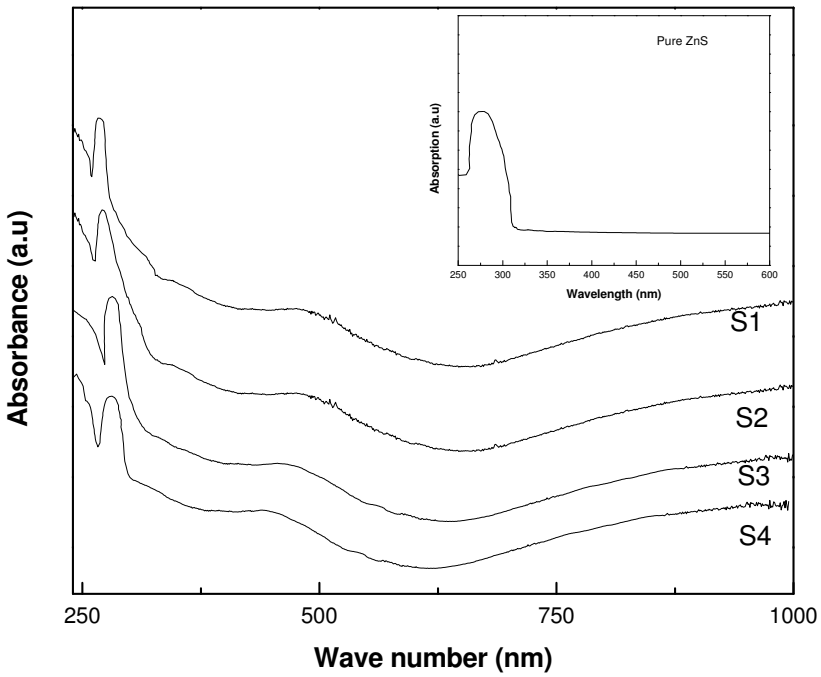

FIG. 6: UV-VIS absorption spectra of the nanocomposite samples S1-S4. The inset represents the same for pure ZnS.

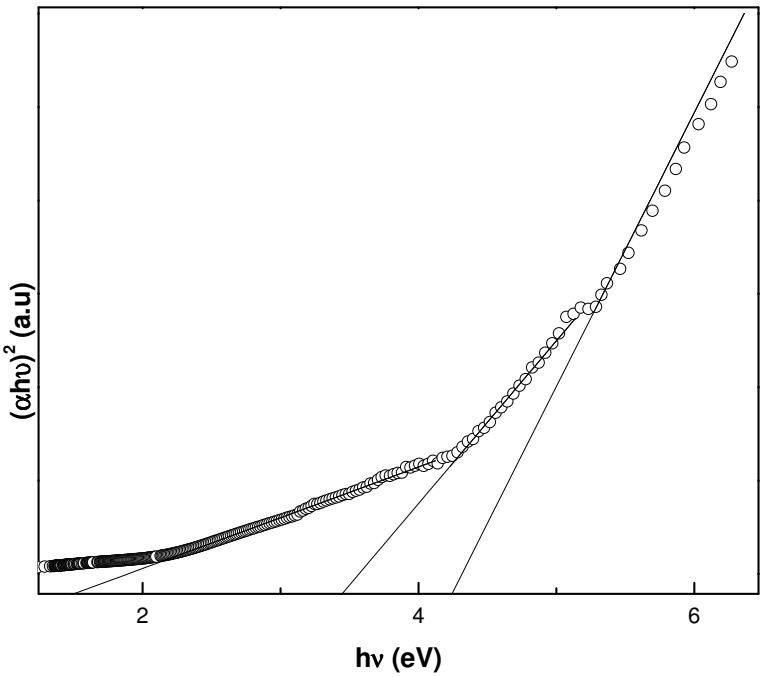

FIG. 7: Plot of $(\alpha\ \mathrm{h}\ \nu\ )^2$ vs. $\mathrm{h}\nu$ for the nanocomposite sample S4 to determine the optical band gap.

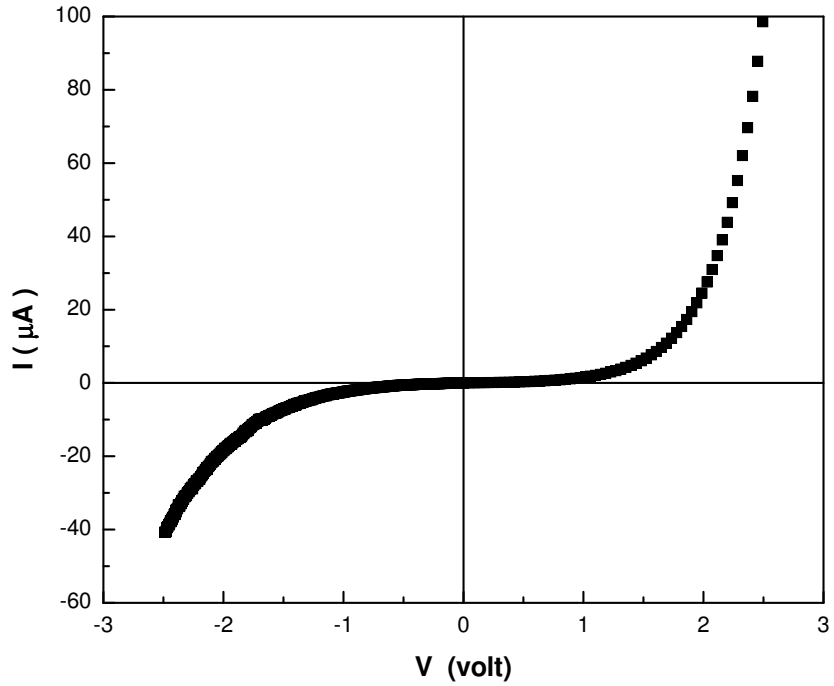

FIG. 8: I-V charecteristics curve for the nanocmposite sample S4.

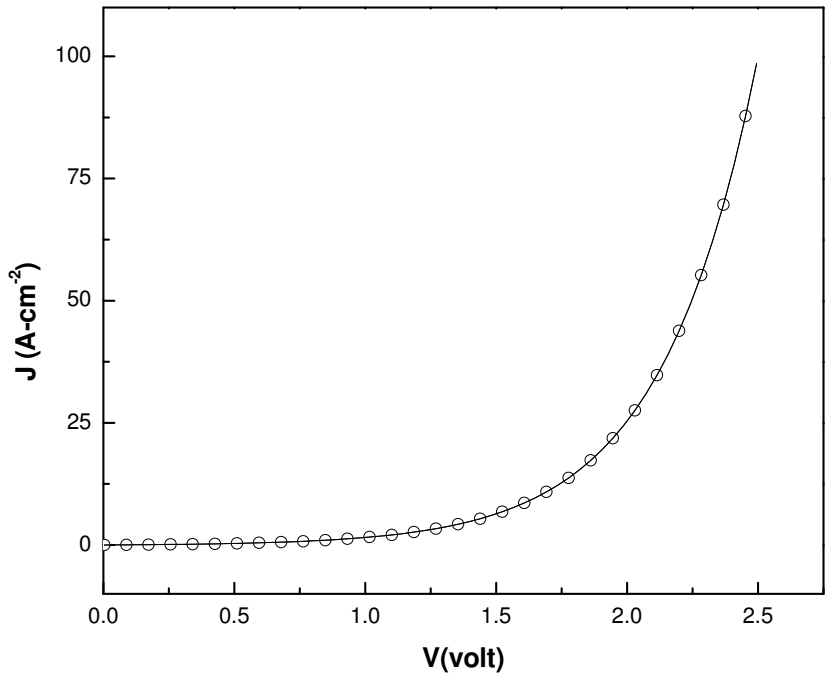

FIG. 9: Forward bias (J vs V) of the nanocomposites sample S4

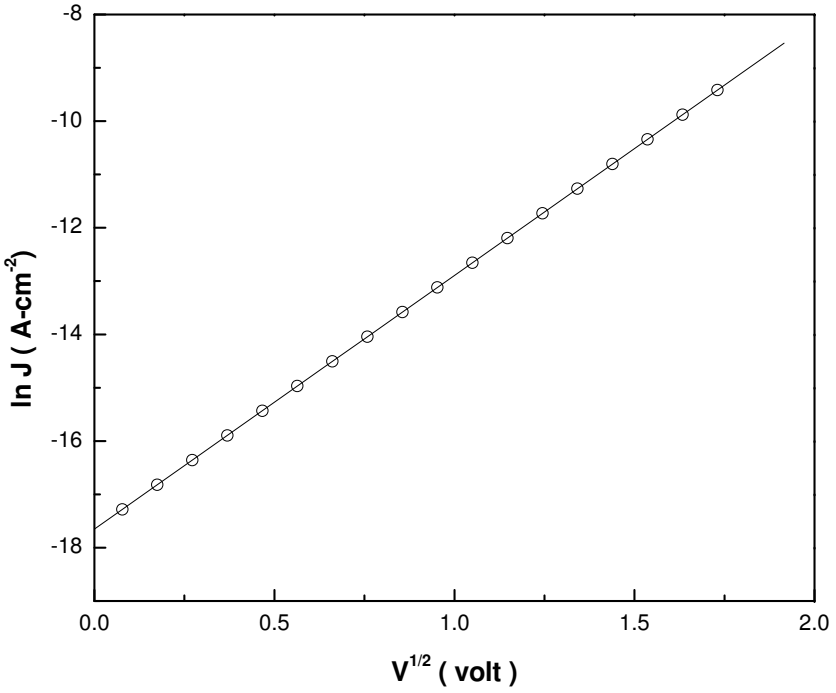

FIG. 10: Reverse bias (ln J vs $V^{1/2}$)of the sample S4.